TECTONICS, VOL. 11, NO. 5, PAGES 944-959, OCTOBER 1992

SEISMICITY AND TECTONICS IN JUJUY PROVINCE, NORTHWESTERN ARGENTINA

Thomas Cahill,[1,2] Bryan L. Isacks,[1] Dean Whitman,[1] Jean-Luc Chatelain,[3] Alejandro Perez,[4] and Jer Ming Chiu[5]

Abstract. The Portable Array for Numerical Digital Analysis (PANDA) network, a digitally recorded seismic array, operated for nine months in Jujuy province of northwestern Argentina. The network was deployed along the eastern edge of the Altiplano-Puna plateau in a major N-S thrust belt that is transitional in style between the thin-skinned deformation of the Bolivian foreland to the north and basement-involved deformation of the Pampean region to the south. Teleseismic locations of crustal earthquakes in the region indicate that seismicity is associated with compressional structures found near the eastern deformation front. No crustal seismicity was detected beneath the Puna plateau to the west. Peak seismicity levels beneath the foreland occurred between 20 and 25 km depth; a sharp decrease in seismicity was observed below 25 km. A estimate of 42 km for the thickness of the Jujuy foreland crust was inferred from wide-angle Moho reflections observed on the digital seismograms. The highest concentration of crustal seismicity was located beneath Sierra de Zapla, a broad anticline immediately east of San Salvador de Jujuy. Many of the earthquakes in the 20-25 km depth range have a shallow, west dipping nodal plane as does the focal mechanism solution for a moderately large 1973 earthquake. Inversion of focal mechanism data for the orientation of principal stresses shows that maximum compression is oriented at azimuth 74°, closely paralleling both the current Nazca-South America convergence direction and the shortening direction derived from regional Quaternary fault slip data. We interpret the earthquakes as occurring on planes of weakness first produced during Cretaceous rifting and later reactivated by Neogene compressive stresses. Crustal seismicity patterns and fault plane solutions suggest the presence of a midcrustal detachment, along which significant late Cenozoic E-W shortening has occurred.

[1]Institute for the Study of Continents and Department of Geological Sciences, Cornell University, Ithaca, New York.

[2]Now at Engineering Tectonics, Winston-Salem, North Carolina.

[3]Office de la Recherche Scientifique et Technique Outre-Mer, IRIGM-LGIT, Universite J. Fourier, Grenoble, France.

[4]Instituto de Minería y Geología, Universidad Nacionál de Jujuy, San Salvador de Jujuy, Argentina.

[5]Center for Earthquake Research and Information and Memphis State University, Memphis, Tennessee.

Paper number 92TC00215.
0278-7407/92/92TC00215$10.00

INTRODUCTION

The foreland of the central Andean cordillera, between latitudes 23°S and 28°S, is part of a major fold and thrust system that formed in response to compressive stresses induced by the convergence of the Nazca and South American plates. Neogene structures and active crustal seismicity are evidence that the thrust belt, situated along the eastern margin of the Altiplano-Puna plateau, is the locus of the most recent tectonic activity in this region of the Andes [Chinn and Isacks, 1983; Jordan et al., 1983]. This segment of the Andean back arc has been described as a region of transition between thin-skinned deformation observed in the Bolivian Subandes to the north and the basement-involved deformation of the Pampean ranges to the south [Jordan et al., 1983; Allmendinger et al., 1983].

Together with the Altiplano plateau of Peru and Bolivia, the Argentine Puna plateau dominates the physiography of the central Andes. The origin of the plateau uplift has been extensively debated. Many recent investigators have been able to confirm and quantify the significant amounts of crustal shortening along the eastern margin of the plateau [Mingramm et al., 1979; Allmendinger et al., 1983; Lyon-Caen et al., 1985; Sheffels et al., 1986; Roeder, 1988; Grier, 1990]. Earlier models of a plateau constructed by additions of magma to its western flank combined with compressive shortening to the east [e.g. James, 1971] have been contested by models that present crustal compression and shortening as dominant elements across the entire breadth of the plateau [Suárez et al., 1983; Isacks, 1988; Wdowinski, 1989]. While only detailed structural studies can resolve the chronology of prior shortening episodes, the extent of crustal thickening as well as the nature of the active mechanisms of this thickening may be approached through seismic techniques. Studies of the spatial pattern of seismicity and of the orientation of tectonic stresses inferred from earthquake focal mechanisms are important first steps in the investigation of crustal deformation and structure.

In August 1988, the Portable Array for Numerical Digital Analysis (PANDA) seismic network was deployed in the Argentine province of Jujuy, east of the Puna plateau (Figure 1). The PANDA system was the first seismic network in this area capable of recording and locating microearthquakes, and thus it offered the first opportunity to study the relationship between seismicity and the actively uplifting mountain ranges of the Santa Barbara system and Eastern Cordillera of NW Argentina.

In addition to microearthquake locations, we present focal mechanism solutions for 30 crustal events and invert these solutions for the orientation of principal stresses in the region. Also included in this study are analyses of wide-angle reflections from the base of the crust, from which the crustal thickness in the Jujuy area is estimated, and a comparison of the focal depths of Jujuy earthquakes with those from the Argentine foreland overlying the subhorizontal slab. Finally, the seismicity pattern and focal mechanisms are combined with local geologic structure in an interpretation that calls for the reactivation of a Cretaceous rift and its midcrustal basal detachment.

REGIONAL GEOLOGY AND TECTONICS

The association between the dip of the subducted Nazca plate and the types of deformational and morphologic

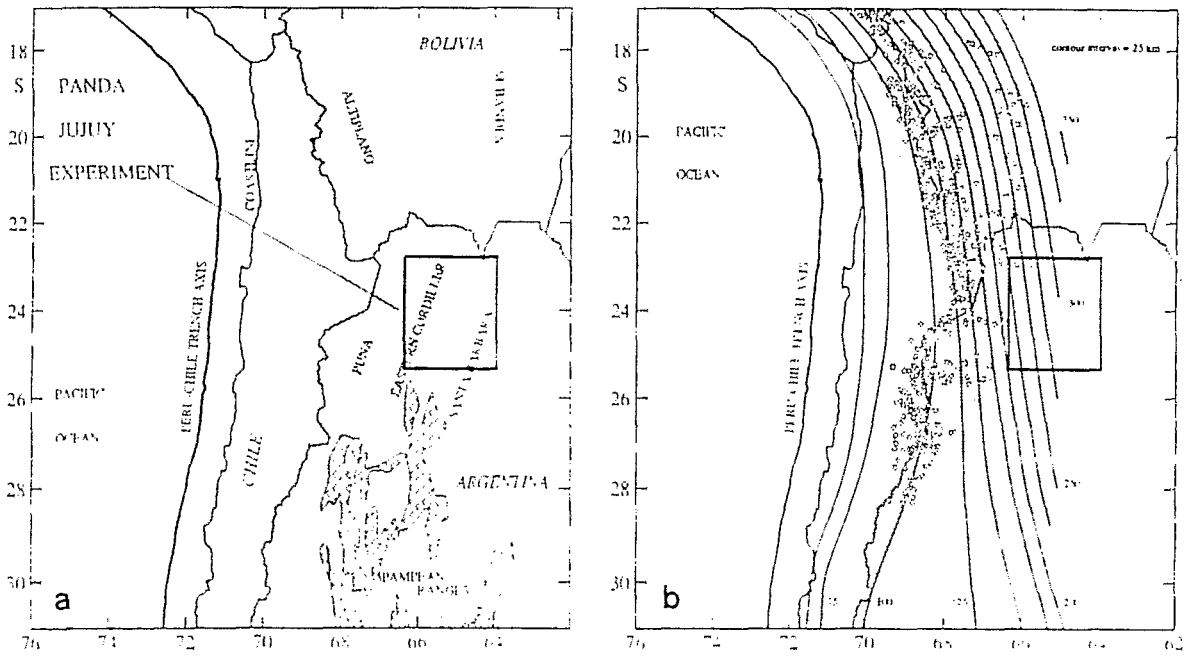

Fig. 1. (a) Map showing location of PANDA network with respect to the major tectonic and physiographic features of the central Andes. Local geologic and topographic structures in this region suggest the area is transitional between classical Subandean thin-skinned fold and thrust belt to the north and thick-skinned deformation seen farther south in the Pampean Ranges. (b) Map showing position of Wadati-Benioff zone contours with respect to the same tectonic and physiographic features of the central Andes shown in Figure 1a [Cahill and Isacks,1990]. The Jujuy experiment took place above the 30°-dipping slab being subducted beneath northwestern Argentina. There is a strong spatial correlation between the more steeply dipping portions of the subducted slab and the presence of active volcanism (open circles) and a high plateau (shaded area) in the overriding South American plate. Beneath northwestern Argentina the 100 and 125 km contours begin to diverge, indicating the formation of a bench that broadens gradually to the south. As the geometry of the subducted slab becomes dominated by this flattened bench south of 28°S, the plateau narrows rapidly, active volcanism ceases, and thick-skinned structures appear in the foreland.

structures seen in the overriding South American plate has been described by many authors [e.g., Barazangi and Isacks, 1976; Jordan et al., 1983; Bevis and Isacks, 1984]. Beneath southern Bolivia the subducted slab dips eastward at an angle of 25°-30° (Figure 1b). Immediately to the south, beneath northwestern Argentina, a horizontal bench appears in the Wadati-Benioff seismicity at a depth of 100 km. The flattening of the subducted slab is manifested in the divergence of the 100 km and 125 km depth contours. The flat bench gradually broadens southward as the slab geometry transforms to assume a subhorizontal form.

Roughly coincident with the change in dip angle of the subducted slab is a change in the style of foreland deformation. North of 23°S, above the "steeply" subducting slab, a classic thin-skinned thrust belt parallels the eastern margin of the southern Altiplano. The west dipping thrust faults of this, the Bolivian foreland belt, cut through a thick sequence of middle Paleozoic and younger rocks and are presumed to sole into a basal detachment [Mingramm, 1979; Allmendinger et al., 1983]. South of 26°S, above the flattening Wadati-Benioff zone, the Andean foreland is dominated by the Pampean ranges, a series of Laramide-type mountains uplifted along reverse faults that bring Precambrian crystalline basement as much as 3 km above the floors of the surrounding basins.

The PANDA network was deployed in the Santa Barbara ranges and Eastern Cordillera of southern Jujuy and northern Salta provinces, in the region of southward thinning pre-Cenozoic basins (Figure 2). In this area, a relatively thin and irregular section of Paleozoic and Mesozoic strata overlies a basement composed of mechanically weak low-grade metamorphic rocks, and a complex system of faults and folds has resulted [Jordan et al., 1983; Allmendinger et al., 1983]. The late Cenozoic tectonic history of the Jujuy segment of the back arc is marked by the persistent eastward migration of the compressional deformation front. The Puna plateau is composed of many internally drained basins that lie at an average elevation of 3.65 km [Isacks, 1988] and are bounded by ranges built primarily through volcanism and reverse faulting during the late Miocene [Turner and Mendez, 1979; Coira et al., 1982; Marrett, 1990]. Although most of the compressional deformation in the Puna ceased by late Miocene, modern faults scarps are common in the eastern Puna [Marrett et al., 1989]. The Eastern Cordillera, at the latitude of Jujuy, is distinguished from the Puna more

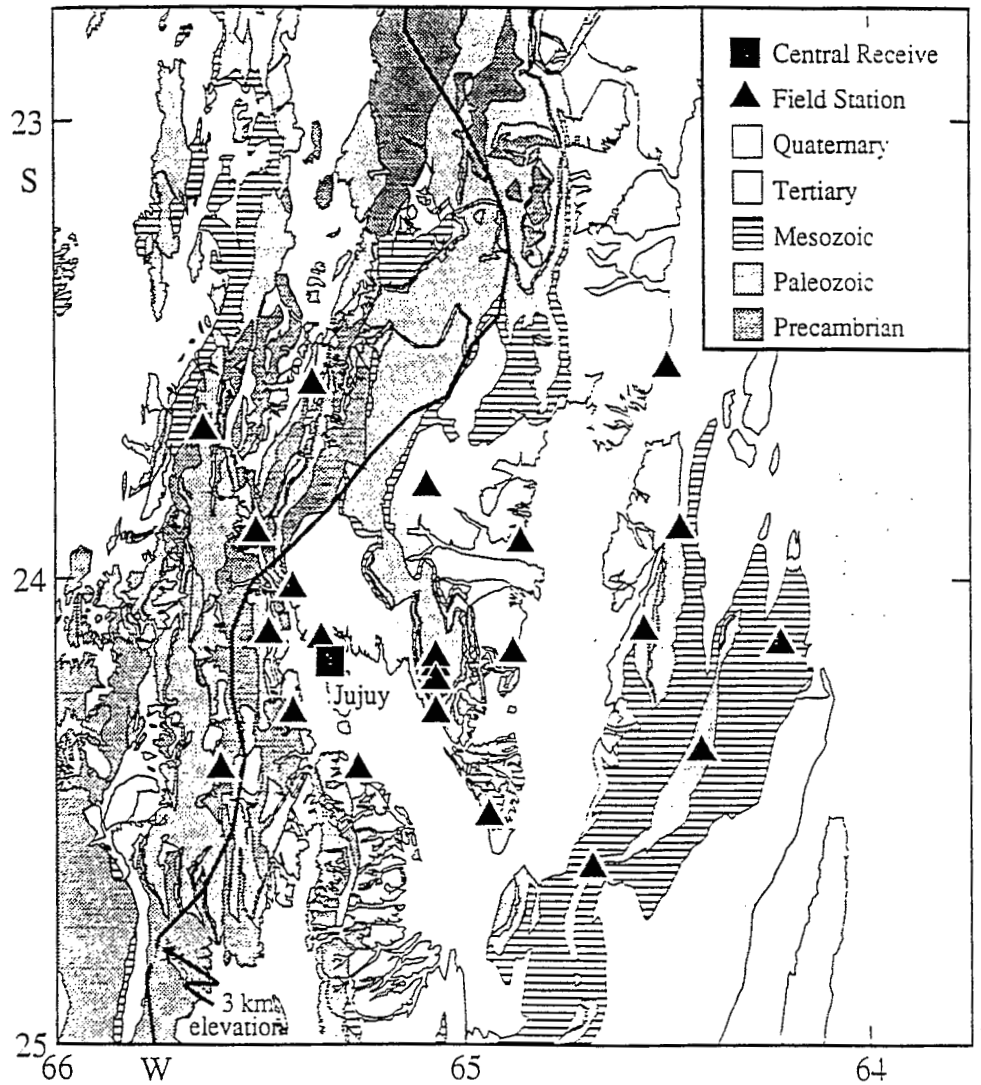

Fig. 2. Map showing locations of the 23 stations deployed in the Eastern Cordillera and Santa Barbara system. The heavy black line indicates the position of the average 3-km elevation contour. The lithologic expression of the relation between structure and topography is seen in the contact placing Precambrian low-grade metamorphic rock over Tertiary strata along the eastern margin of the Eastern Cordillera, which roughly parallels the 3 km contour.

by its relief than by any fundamental differences in structural style or lithology. The eastern wall of the Cordillera represents the topographic slope separating the high plateau from the lower ranges of the foreland to the east. The Eastern Cordillera was uplifted about 10-12 Ma, during the late Miocene Quechua stage of deformation [Russo and Serraiotto, 1979; Coira et al., 1982], primarily along N-S striking reverse faults that bring lower Cambrian and Precambrian low-grade metamorphic rocks to the surface [Jordan and Alonso, 1987]. Farther east, the deformational structures that dominate the Santa Barbara ranges are broad, elongate anticlines cored by early Paleozoic strata and bounded on one or both flanks by N-S striking reverse faults [Jordan et al., 1983]. The deformation of the Santa Barbara system appears in general to have begun later than in the Eastern Cordillera [Russo and Serraiotto, 1979], however active shortening of both provinces is indicated by thrust faults cutting Quaternary alluvial structures [Jordan et al., 1983; Salfity et al., 1984].

HISTORICAL AND TELESEISMIC DATA

The region of northwestern Argentina that today comprises Jujuy province and northeastern Salta province has throughout historical times suffered large, often destructive earthquakes (Figure 3). Historical activity is concentrated near the eastern deformation front in the Santa Barbara ranges and southern Subandean belt [Castano, 1977]; the lone exception is the 1930 La Poma earthquake, whose reported magnitude of 6.0 [Gutenberg and Richter, 1954] may have been substantially overestimated [R. Marrett, personal communication, 1990]. The five teleseismically located earthquakes with the largest body wave magnitude (mb > 5.5) have also

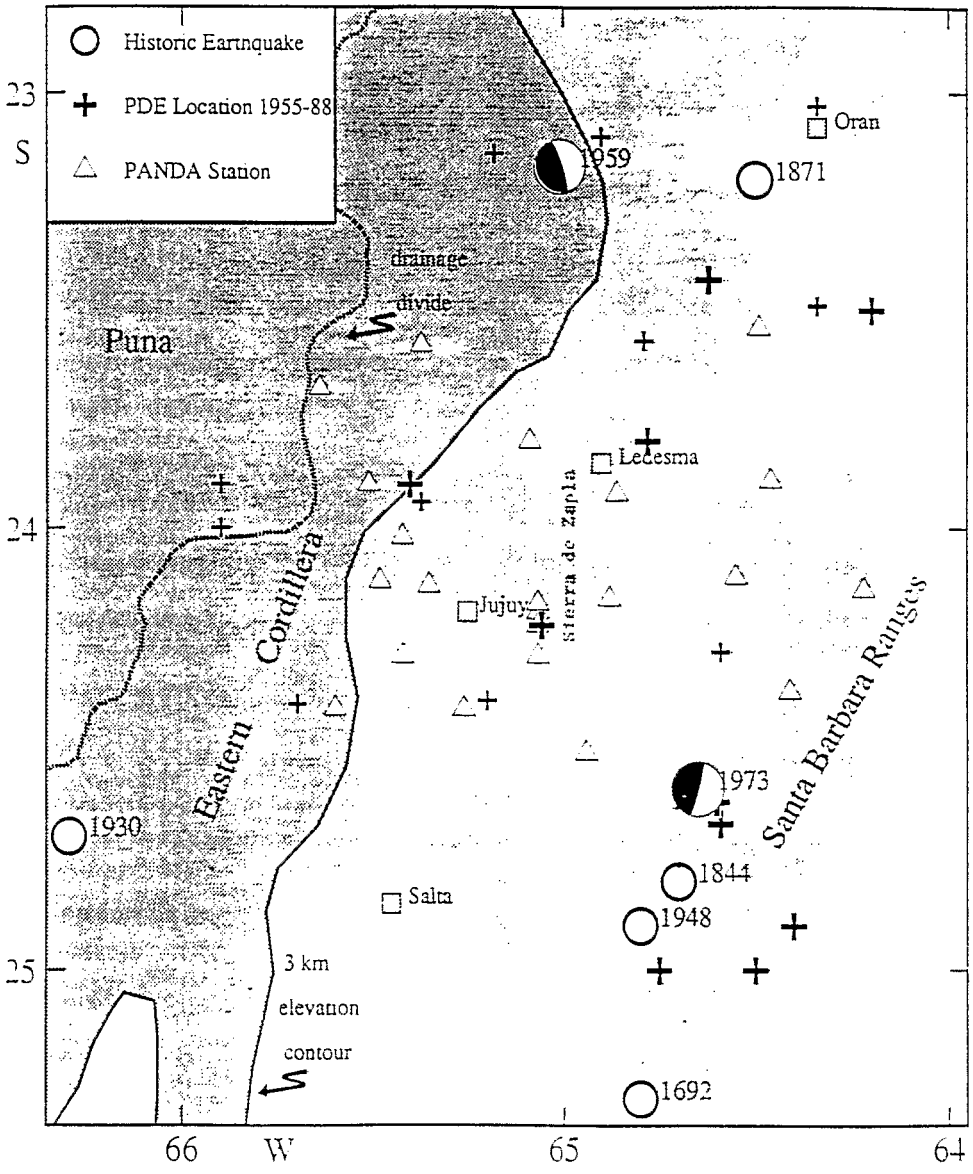

Fig. 3. Map showing historical and teleseismically recorded crustal earthquakes in the study area. The locations of all moderate to large historical events (mb > 6.0 or MM > VI) and all events recorded by 15 or more stations of the global seismograph network (corresponding roughly to events mb > 4.5) are shown. Both the teleseismic events (from the Preliminary Determination of Epicenters catalog 1955-1988) and the historical activity [from Castano, 1977] are concentrated in the eastern part of the foreland, near the deformation front of the central Andes.

occurred in the east, including the 1959 mb = 6.8 earthquake west of the city of Oran.

Focal mechanism solutions for the 1959 and the 1973 (mb = 5.6) earthquakes have been obtained from body wave modeling of long-period seismograms [Chinn and Isacks, 1983; J. Masek, unpublished manuscript, 1989]. The fault plane solutions for both events indicate E-W compressive stresses in the area (Figure 3), which is consistent with both the style and orientation of the fold and thrust belt. Chinn and Isacks [1983] placed the 1959 earthquake at a depth of 12 km, with an epicenter very near the position of the principal thrust that separates the Eastern Cordillera from the southernmost extent of the Subandean belt.

PANDA SEISMIC NETWORK AND DATA

Network Description

From August 1988 to April 1989, a network of 23 portable seismic stations was deployed within the Eastern Cordillera and Santa Barbara ranges of Jujuy province. Final network dimensions reached 145 km by 120 km, with interstation spacings ranging from 3 km to 45 km. The geographic position of each station was obtained using a global positioning system (GPS) receiver, which provided both station elevations and geographic coordinates with an accuracy of 15 m.

Each field station employed two three-component, 4.5-Hz seismometers. One seismometer signal was sent through a

high-gain amplifier, the other through a low-gain amplifier, providing a recording system with 90 dB of dynamic range. The amplified signals were multiplexed and telemetered to the Instituto de Minería y Geología in San Salvador de Jujuy, where the signals were processed through a central receiving unit, trigger detection system, analog-to-digital converter, and digital recorder.

Hypocenter Location Method

Arrival times of P and S waves were picked using an interactive seismogram display program. The combination of high sampling rate and display flexibility allowed the routine picking of P arrivals to an accuracy of 0.03 - 0.05 s; impulsive P arrivals were picked with an accuracy of 0.01 - 0.02 s. The typical accuracy range for S arrivals was 0.1-0.5 s, with impulsive arrivals picked with considerably higher accuracy.

Earthquakes were located using the program HYPOINVERSE [Klein, 1985]. The crustal velocity structure in the area of the network was not known prior to this experiment. Some shallow depth ($h < 10$ km), localized velocity information was available in the form of interval velocities derived from seismic reflection data gathered by Yacimientos Petroliferos Fiscales, the Argentine national oil company. A preliminary model was constructed using published geological cross sections and isopach maps [Mingramm et al., 1979; Salfity, 1979] as guides for shallow ($h < 10$ km) structure. The velocity of deeper crustal layers was estimated by plotting apparent P wave velocity (Vp) versus distance. S wave velocities (Vs) were estimated by determining the Vp/Vs ratio from Wadati plots.

Initial station delays used in HYPOINVERSE were computed as combinations of altitude and basin corrections. Using the preliminary HYPOINVERSE locations of events with good station distributions and small error statistics, arrival times for events of various depths were matched with travel time curves derived from the original velocity model. Adjustments were made to the preliminary velocity model by two methods: (1) for shallow layers traversed by many ray paths ($h < 25$ km) a two-dimensional velocity inversion program developed by Roecker [1982, 1987] was used to adjust both velocities and station corrections and (2) for deeper layers, with insufficient penetration by seismic rays to allow application of the inversion technique, forward travel time modeling was used. Velocities of the lower layers were adjusted iteratively along with relocation of the microearthquakes until a satisfactory fit between the observed travel time data and synthetic travel time curves generated from the model was achieved. Table 1 shows the final velocity model used in locating the local events.

The crustal earthquakes were classified according to the reliability of their hypocentral location by using error statistics supplied by HYPOINVERSE (Table 2). Earthquakes within or immediately adjacent to the network consistently had more reliable locations. The large aperture of the network, however, allowed good epicentral determinations for events outside the network (epicentral error estimate ≤ 2.0 typically for events with five or more P arrivals), even though depth estimates for these events were poor.

PANDA RESULTS

Crustal Thickness in the Jujuy Foreland

Seismograms produced by crustal events that occurred near the edge of the network were carefully examined for all secondary arrivals, and particularly for reflections off the base of the crust. The reflection geometry shown in Figure 4 was generated by inserting the crustal velocity model into a ray tracing program developed by Luegert [1988]. Only those crustal earthquakes near the boundaries of the network were sufficiently removed from the far side of the array to permit reception of critical angle to wide-angle Moho reflections, while being close enough for an accurate determination of hypocenters. For events with focal depths between 10 and 15 km, critical angle to wide-angle reflections are first seen at stations almost 100 km away. Deeper foci would decrease the offset needed for critical angle reflections. In the Jujuy area, however, those deeper events ($h = 20$-25 km) were found only near the center of the array and thus were of no use for this study.

Hypocenters and origin times for crustal earthquakes near the edge of the network were determined, and record sections were constructed from the digital traces (Figure 5). The traces were time shifted to correct for computed station delays and then matched to synthetic travel time curves generated from the Jujuy crustal velocity model. A strong secondary arrival, identified as the Moho-reflected P wave,

TABLE 1. Velocity Model Derived From Inversion of Travel Times of Well-Located Crustal Earthquakes

Layer	P Velocity km/s	S Velocity km/s	Depth to Top of Layer, km
1	3.98	2.34	0
2	5.28	3.10	3
3	6.21	3.65	10
4	6.45	3.79	20
5	6.80	4.00	35
6	8.00	4.70	42

TABLE 2. Grading Critertia Applied to Jujuy Crustal Earthquakes

Grade	P	S	ERH, km	ERZ, km	RMS, s	CN	No. of Events
A	4	4	0.5	0.75	0.15	25.	39
B	3	3	1.0	1.50	0.25	50.	98
C	2	2	2.0	5.00	0.35	100.	46
D	3	-	-	-	-	-	160

P is the minimum number of P wave arrivals, S is the minimum number of S wave arrivals, ERH is the epicentral error estimate, ERZ is the focal depth error estimate, RMS is the rms travel time residual, and CN is the condition number.

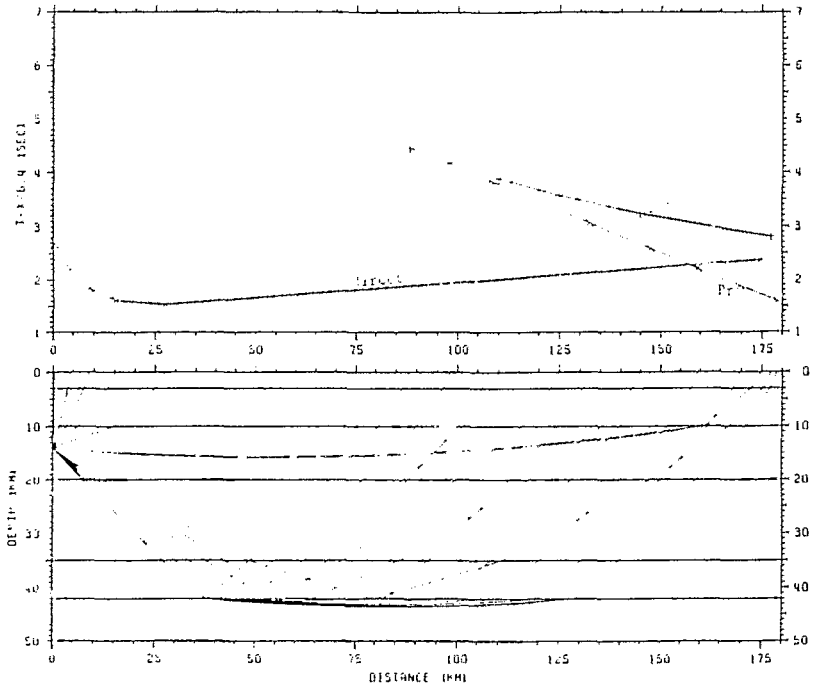

Fig. 4. Plots showing geometry of Moho reflections (bottom) and synthetic travel time curves (top). The reflection geometry was generated by inserting the Jujuy crustal velocity model into a ray tracing program [Luetgert,1988]. Events with h = 10-15 km have critical angle to wide-angle reflections at distances greater than 85 km.

PmP, is seen at near-critical to postcritical distances in both examples shown in Figure 5. The delay between the arrival of the direct P wave and the arrival of PmP indicates a crustal thickness of 42 km ± 3 km.

Reflection points on the Moho for the two examples shown in Figure 5 were determined from the reflection geometry and plotted in map view (Figure 6). The crustal thickness estimate of 42 km applies to the area near the east flank of the Sierra de Zapla anticline. Constraints on the position of Moho at other locations are being obtained by an examination of apparent velocities and station delays observed on PANDA recordings of intermediate-depth earthquakes beneath the plateau [Whitman et al., 1989].

Seismicity Patterns

Over 300 crustal microearthquakes were recorded during the nine months of network operation in Jujuy, along with hundreds of intermediate-depth events in active clusters of the central Andean Wadati-Benioff zone. Most of the crustal microearthquakes recorded were located near two roughly N-S striking ranges of the foreland, the Sierra de Zapla anticline and the Santa Barbara range (Figure 7). A small cluster of earthquakes was detected in the southern Subandean belt west of the city of Oran (23.0°S, 64.6°W), near the site of the 1959 earthquake. Sparse seismic activity was also detected south and east of the network in

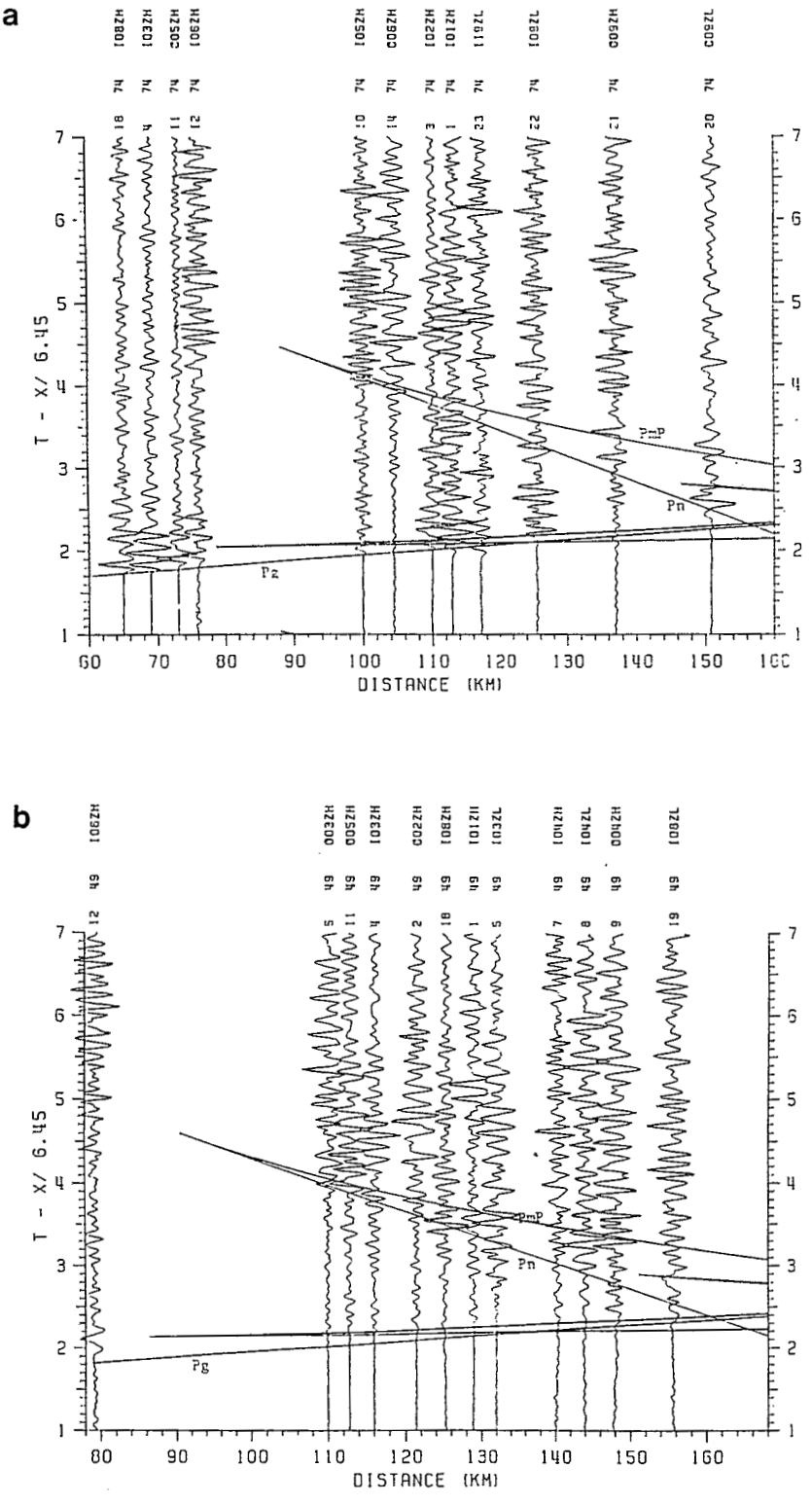

Fig. 5. Record sections constructed from the digital traces for two crustal earthquakes located near the edge of the PANDA network. The traces were band pass filtered (0.01-10 Hz) and time shifted to correct for computed station delays. Synthetic travel time curves generated from the Jujuy crustal velocity model are superimposed on the seismograms. A strong secondary arrival identified as the Moho-reflected P wave, PmP, is seen at near-critical to postcritical distances in both examples. The delay between the arrivals of the direct P wave and PmP indicates a crustal thickness of about 42 km.

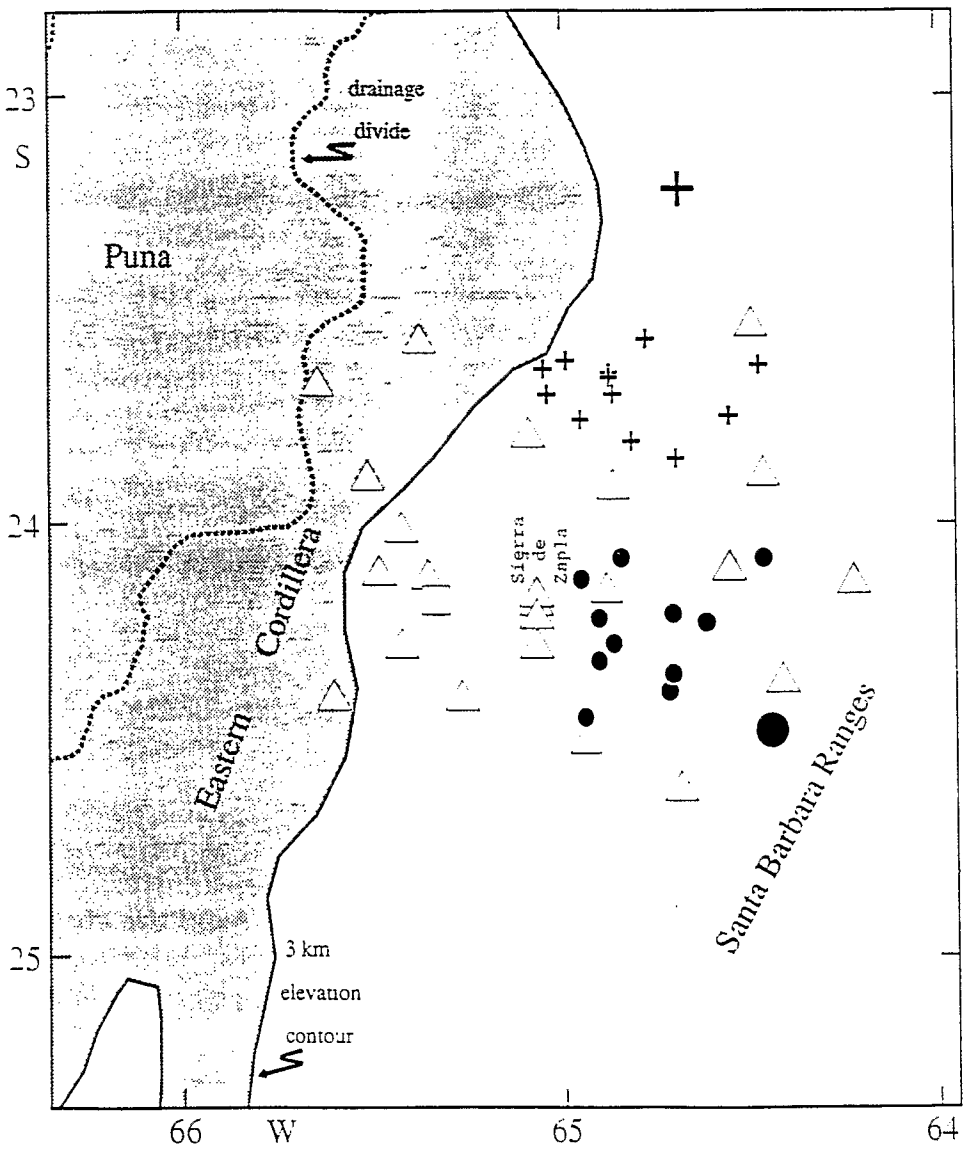

Fig. 6. Map showing surface projection of Moho reflection points for the two crustal earthquakes shown in Figure 5. Large symbols denote epicenters of the two events; reflection points, denoted by the smaller symbols, were determined from the ray tracing geometry shown in Figure 4. The crustal thickness estimate of 42 km is confined to the area near the east flank of the Zapla anticline. This value is used to constrain the position of Moho in Figure 12.

the eastern Santa Barbara ranges. Although a few events immediately west of the network in the Eastern Cordillera were also recorded, the crust of the Puna plateau was aseismic during the experiment. Difficulty in establishing telemetry links between the high plateau and the central receiving site in San Salvador de Jujuy prevented the installation of network sites on the plateau. Two short experiments were conducted on the Puna with portable seismographs, with a total of 6 days of analog data recorded. These short-duration experiments also failed to record crustal activity in the Puna, confirming the conclusion based on teleseismic and PANDA network data that the plateau near 24°S latitude is an area of very sparse seismic activity.

The highest concentration of crustal seismicity was located beneath the broad Sierra de Zapla anticline. located immediately east of San Salvador de Jujuy (Figure 7). This anticline, along with the anticlinal Santa Barbara ranges farther east, are the northernmost indications of the north-to-south change in structural style of the Andean foreland from thin-skinned folding and thrusting to basement-involved block faulting. The epicenters of many microearthquakes form short, linear segments that may correspond to the fault segments bounding the uplifts. One of these faults is seen at the surface on the eastern flank of the anticline (23.9°S, 64.9°W) and along the contact between Tertiary and older units near 24°S on the western flank of Sierra de Zapla.

The distribution of microseismicity and its relationship to surface topography are shown more clearly in cross section (Figure 8). Seismicity at depths less than 15 km is concentrated near the flanks of the Sierra de Zapla

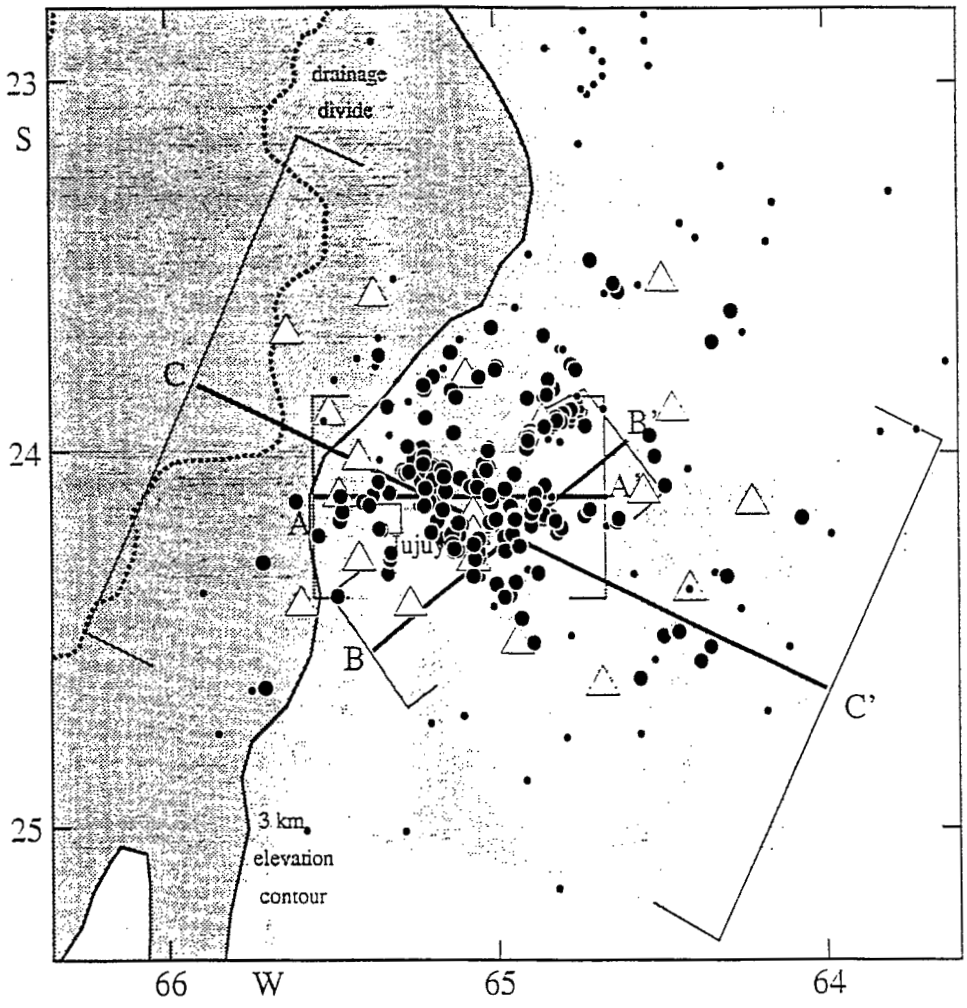

Fig. 7. Map showing epicenters of crustal earthquakes (solid circles) recorded by the network. Larger circles represent events having more reliable locations. Seismicity is concentrated beneath the Zapla anticline east of the city of San Salvador de Jujuy. Microearthquakes were also located in the southernmost Subandean belt, the Santa Barbara Ranges, and the easternmost Eastern Cordillera; no seismicity in the crust of the Puna was detected during this period. Heavy lines indicate positions of cross sections shown in Figure 8.

anticline, and continues diffusely westward beneath the Eastern Cordillera. Two lineations in the recorded crustal seismicity appear to be directly associated with faults mapped at the surface. The first, seen in cross section as a tight knot near 10 km depth in on the eastern flank of the anticline (Figures 8a and 8c) formed during a 2-day aftershock sequence following one of the larger-magnitude crustal events recorded by the network (mb ≈ 4.0). These events occurred below and slightly west of a N-S scarp visible on satellite imagery. The second lineation is a deeper, east dipping plane of microearthquakes, between depths of 10 and 25 km, that projects to the surface at a faulted contact between Tertiary and lower Paleozoic strata on the southwest limb of the anticline (Figure 8b).

Most of the crustal microseismicity recorded by the PANDA network occurred at depths between 20 and 25 km beneath Sierra de Zapla. The slight westward dip of the deeper seismicity can be seen in the narrower section (Figure 8a), though it is blurred somewhat when events from a wider area are included (Figure 8b). A discussion of the relationship between seismicity and regional-scale geologic structures follows presentation of focal mechanism data.

Regional Stress Orientation

Focal mechanism solutions for 30 of the larger and more precisely crustal events were obtained using P waves first motion polarities and the program FPFIT [Reasonberg and Oppenheimer, 1985] (Table 3). An average of 14.3 first motions were used to determine solutions for individual events, with 0.8 discrepant polarities per event. The mean errors in dip direction, dip, and rake were 6.9°, 7.0° and 9.6°, respectively. Although the orientation of fault planes and sense of slip vary considerably for the crustal microearthquakes, some consistent patterns are recognized. The majority of events contain a shallowly plunging east-west oriented P axis, indicating predominant E-W

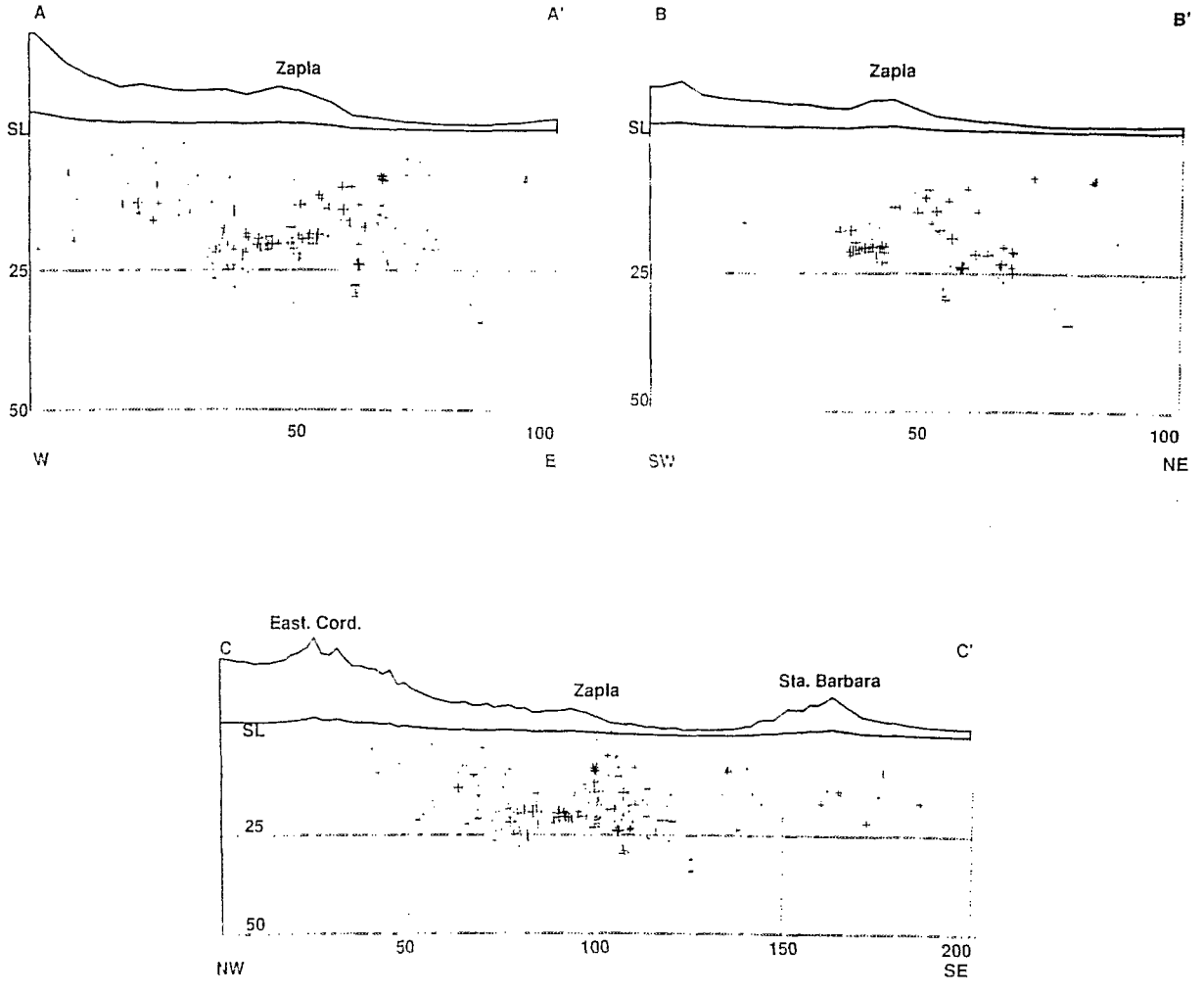

Fig. 8. Cross sections through seismicity along profiles shown in Figure 7. Larger crosses indicate the location of events with more reliable solutions. Sections A-A' and B-B' show details of the seismicity beneath central and southern portions of Zapla anticline, respectively. Microearthquakes at shallower depths are located near the flanks of the anticline, while activity at 20-25 km runs beneath the entire structure. Section C-C' shows seismicity projected onto a vertical plane normal to the regional trend of tectonic structures. Along with the high level of seismicity beneath the Zapla anticline and scattered activity beneath the Santa Barbara Ranges, several events can be seen near the eastern margin of the Eastern Cordillera, a major zone of thrusting.

shortening (Figure 9). Shallow events found near the margins of the Zapla-Centinela anticline generally have either high-angle reverse fault mechanisms (events 4, 16, 17, 19) or strike-slip mechanisms with a substantial thrust component (events 11, 14, 20, 24). Deeper events (h = 20-25 km) have more varied solutions but typically have one nodal plane with a shallow dip to the west (events 3, 6, 9, 13, 27, 28, 29).

To examine the stress field in the Jujuy area, the focal mechanism data were inverted for regional stress orientation using the method developed by Gephart [1990]. For the Jujuy foreland, the best fit maximum compression axis ($\sigma 1$) is found at azimuth 74°, plunge 32° ENE; the corresponding minimum compression direction ($\sigma 3$) is at azimuth 242°, plunge 50°WSW (Figure 10). The best fit "R value", where $R = (\sigma 1 - \sigma 2)/(\sigma 2 - \sigma 3)$, is 0.4, indicating that the magnitude of $\sigma 2$ is roughly intermediate between $\sigma 1$ and $\sigma 3$. These results are consistent with the intuition that the N-S striking fold and thrust belts in the region result from the application of roughly E-W compressive stresses. Furthermore, the azimuth of maximum compressive stress (74°) obtained in the inversion is similar to both the azimuth of Nazca-South America plate convergence at this latitude (78°) [Pardo-Casas and Molnar, 1987; Pilger, 1984] and the shortening direction derived from Quaternary fault-slip data near the study region (65°) [Marrett, 1990].

Focal Depths

Accurate focal depths were obtained for 133 earthquakes that occurred within the bounds of the network. A

TABLE 3. Focal Mechanism Solutions for Jujuy Crustal Earthquakes

	Date	Time, GMT	Latitude	Longitude	Depth, km	Pole 1 az	Pole 1 pl	Pole 2 az	Pole 2 pl	T az	T pl	P az	P pl	B az	B pl	FPFIT stns	FPFIT discr	FPFIT Errors direction	dip	rake
1	Nov. 26, 1988	1438	-24° 9.66'	-64° 43.26'	29.83	270	35	146	39	211	58	117	02	26	32	12	1	3	8	5
2	Nov. 30, 1988	1720	-24° 8.61'	-65° 13.08'	20.49	285	0	195	50	252	33	138	33	15	40	14	1	5	10	15
3	Nov. 30, 1988	2140	-24° 10.03'	-64 56.39'	24.22	265	15	119	72	251	59	93	29	358	10	13	0	20	5	25
4	Dec. 03, 1988	2323	-23° 58.98'	-65° 13.22'	13.18	265	10	158	59	234	47	109	29	1	29	15	1	8	5	0
5	Dec. 16, 1988	1828	-24° 6.59'	-65° 1.11'	18.80	290	35	93	54	324	77	103	9	194	8	16	1	3	10	15
6	Dec. 18, 1988	1029	-24° 4.27'	-65° 10.48'	28.21	240	5	124	79	229	49	69	39	331	10	14	0	8	5	30
7	Jan. 11, 1989	0116	-24° 3.29'	-65° 2.61'	18.82	350	75	211	11	223	55	23	33	119	10	18	2	0	8	5
8	Jan. 11, 1989	1137	-24° 19.76'	-65° 4.12'	18.10	50	55	230	35	230	80	50	10	320	0	11	0	10	10	10
9	Jan. 18, 1989	1536	-24° 2.83'	-65° 12.63'	23.17	70	85	290	4	294	49	107	41	200	3	13	1	10	13	10
10	Jan. 23, 1989	2254	-24° 1.70'	-65° 13.75'	23.22	35	40	153	29	100	53	2	6	268	36	15	1	3	3	10
11	Jan. 27, 1989	0607	-24° 8.52'	-64° 57.22'	9.79	355	25	261	9	40	11	305	24	152	63	19	2	3	3	20
12	Feb. 03, 1989	2032	-24° 9.28'	-64° 53.32'	21.32	60	25	263	63	40	68	247	19	154	9	14	1	15	8	10
13	Feb. 08, 1989	0012	-24° 4.03'	-65° 10.76'	21.78	325	10	100	76	337	54	136	34	233	10	13	0	10	5	10
14	Feb. 08, 1989	1150	-23° 49.41'	-65° 12.87'	8.13	145	20	242	19	194	28	103	1	12	62	14	1	8	25	10
15	Feb. 08, 1989	1625	-24° 16.87'	-65° 3.02'	22.63	255	40	90	49	202	81	82	5	351	8	17	2	15	10	10
16	Feb. 12, 1989	2121	-23° 57.01'	-64° 54.08'	7.16	270	50	103	39	147	82	277	5	8	6	17	1	10	5	10
17	Feb. 12, 1989	2235	-23° 57.74'	64° 53.62'	7.70	285	50	80	37	28	76	271	7	179	13	17	1	5	5	15
18	Feb. 12, 1989	2303	-23° 56.26'	-64° 53.02'	17.93	30	20	210	70	210	25	30	65	300	0	12	0	0	0	5
19	Feb. 13, 1989	0236	-23° 56.91'	-64° 53.47'	7.96	350	5	84	40	29	31	134	23	254	50	12	1	3	10	0
20	Feb. 14, 1989	1242	-23° 49.65'	-65° 12.67'	9.38	335	35	77	16	31	37	292	12	187	50	12	0	3	3	5
21	Feb. 16, 1989	0012	-23° 57.48'	-64° 53.46'	8.62	245	50	102	34	266	9	153	69	359	19	16	2	13	5	10
22	Feb. 22, 1989	0413	-23° 40.71'	-64° 50.63'	15.23	260	50	117	34	168	69	281	9	14	19	14	1	5	5	0
23	Mar. 01, 1989	0011	-24° 15.57'	-65° 2.97'	23.46	75	55	337	6	129	31	9	41	243	34	9	0	5	8	5
24	Mar. 06, 1989	0751	-23° 54.06'	-65° 12.29'	19.09	145	10	51	20	7	7	100	21	261	68	13	1	5	10	10
25	Mar. 20, 1989	1349	-24° 12.60'	-64° 56.19'	29.28	15	20	263	46	332	49	223	15	121	37	19	0	5	3	10
26	Mar. 22, 1989	1450	-24° 12.82'	-64° 56.39'	28.83	350	35	226	39	291	58	197	2	106	32	17	1	0	10	5
27	Mar. 25, 1989	2057	-23° 45.47'	-64° 58.98'	23.43	270	85	60	4	242	41	57	49	150	2	14	1	10	3	10
28	Mar. 25, 1989	2121	-23° 45.52'	-64° 59.16'	21.89	280	15	134	72	266	59	108	29	13	10	15	1	5	3	0
29	Apr. 02, 1989	0946	-24° 15.60'	-65° 7.20'	21.74	95	85	325	3	141	42	329	48	235	4	12	1	13	3	10
30	Apr. 03, 1989	2022	-24° 15.53'	-65° 7.15'	21.03	220	0	130	30	179	21	81	21	310	60	11	0	5	10	10

az = azimuth pl = plunge stns = number of stations discr = discrepant polarities

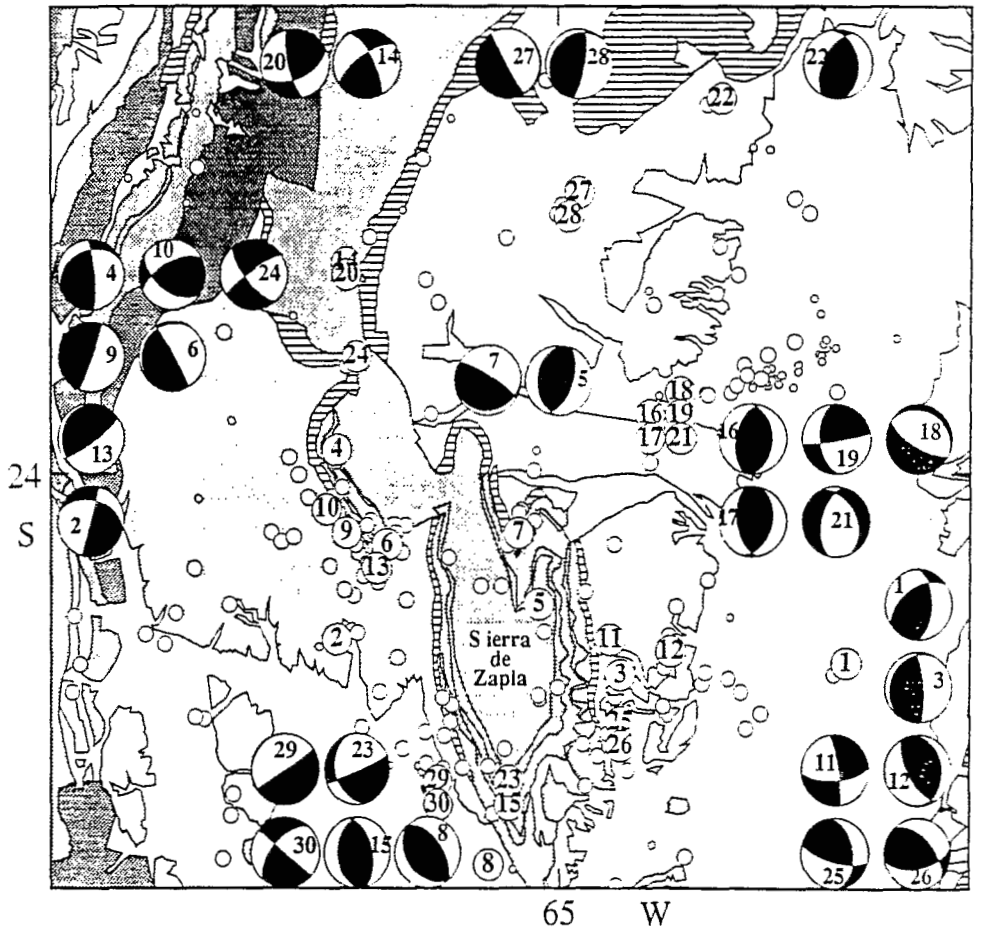

Fig. 9. Lower hemisphere projections of 30 focal mechanism solutions for crustal earthquakes; compressional quadrants are shaded. Epicenters of events having focal mechanisms are plotted as large open circles; index numbers correspond to numbers seen in the unshaded quadrants of each solution and in Table 3, first column. The majority of events have thrust or reverse fault solutions with P axis aligned roughly east-west. There is, however, significant variation in the type of mechanism observed: many reverse faults have a large component of oblique motion, and a normal solution is sometimes seen. Several solutions (3, 6, 9, 13, 27, 28, and 29) from events at 20-25 km depth show a consistent shallow west dipping plane, possibly associated with motion along a detachment. Shallower events commonly have more steeply dipping nodal planes with either reverse or strike-slip motion.

histogram summarizing the depth distribution of these events is shown in Figure 11a. Ninety percent of the microearthquake activity recorded was found between 5 and 25 km depth. A strong peak in the histogram of focal depths is seen between 20 and 25 km, with a very sharp decrease in the number of events below 25 km.

Precise determinations of focal depths for crustal microearthquakes in the Pampean ranges of San Juan Province have been obtained by Smalley and Isacks [1990]. In this region of the Andean foreland, 800 km to the south of Jujuy, the highest concentration of focal depths lies between 25 and 30 km. Substantial activity occurs below 30 km beneath San Juan, and the maximum focal depth is found at 42 km (Figure 11b).

The variation in depth of crustal seismicity in these two regions may be a result of systematic location errors, or it may reflect a difference in composition of rock found at midcrustal levels. Basement rocks exposed at the surface are markedly different in the two regions: the middle and upper crust of the Pampean ranges of San Juan is composed of homogeneous and mechanically strong granitoids and migmatites [Caminos, 1979; Ramos et al., 1986]; in the Jujuy foreland, low-grade metamorphics are the dominant basement rock. A significant lateral variation in the lithology at midcrustal levels could result in different depths to the brittle-plastic transition.

Another plausible explanation for the observed difference in maximum and mean depths of seismicity beneath these two regions may be found in the subducted slab geometry. From the attenuation of high-frequency shear waves, several investigators have inferred the presence of a well-developed asthenospheric wedge above the steeper slab [Barazangi et al., 1975; Whitman et al., 1989]. A higher heat flow through the crust at the eastern edge of the plateau near Jujuy, associated with asthenospheric circulation, could result in a warmer, more ductile lower crust than above the horizontally subducting plate in San Juan.

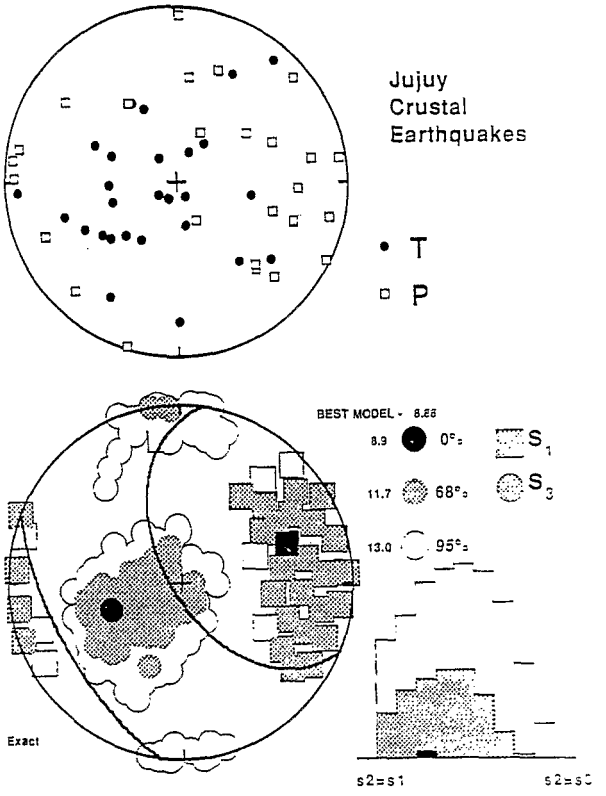

Fig. 10. Results from an inversion of focal mechanism data for the orientation and relative magnitudes of the principal stresses. Maximum compression (denoted by the solid square) is aligned ENE and inclined slightly above the vertical. Minimum compression (denoted by the solid circle) is more nearly vertical and trends WSW. The scatter in P and T axes, seen in the upper portion of the figure, is considerable and may indicate that the assumption of homogeneous stress does not apply for entire Jujuy region.

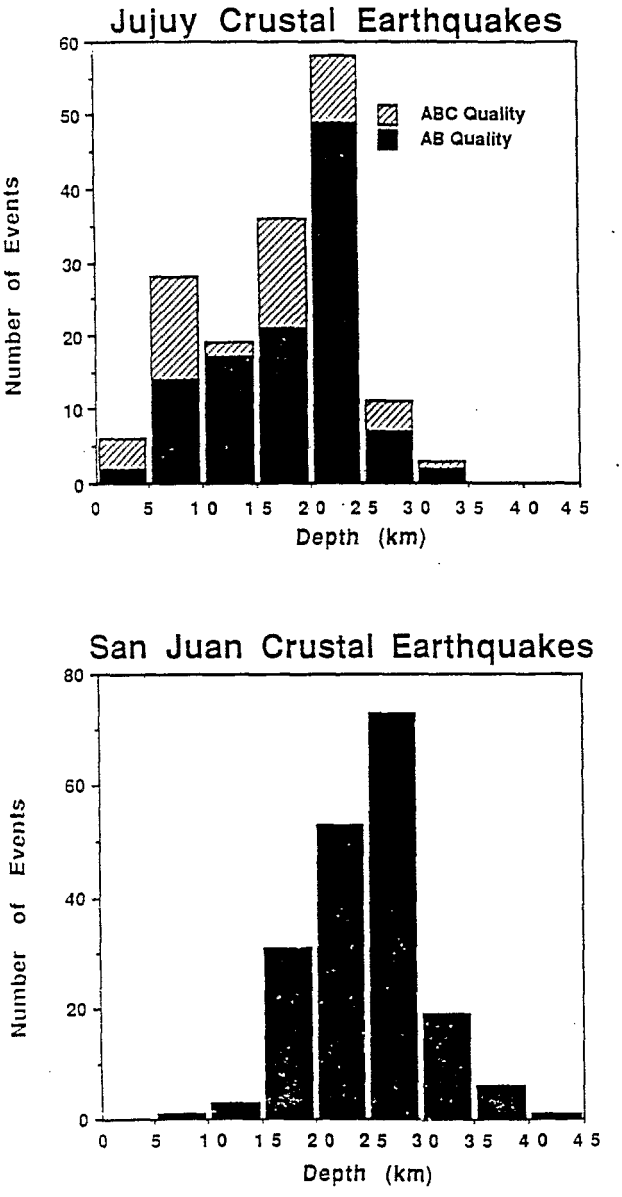

Fig. 11. Depth histograms for Jujuy and San Juan crustal earthquakes. Jujuy events were classified with regard to reliability of their depth solution using location statistics provided by HYPOINVERSE. The Jujuy depth histograms show a strong peak at 20-25 km; while there is considerable activity on faults at shallower levels, the seismicity drops off rapidly below 25 km. San Juan crustal seismicity reaches peak levels between 20 and 30 km, significant activity occurs below 30 km, and the maximum focal depth is 42 km.

DISCUSSION

The spatial correlation of pre-Andean paleogeography with modern slab geometry and structural style is a subject of continued speculation. A likely explanation is that the current rheological and mechanical properties of the foreland crust are a result of both past and present geographic position within a convergent margin setting. While regional scale (long wavelength) tectonic features such as the active magmatic arc, thinned lithosphere, and the uplifted plateau reflect the current tectonic setting, the localized (short wavelength) mode of upper crustal deformation depends more on near- surface preexisting conditions, such as the presence or lack of a sedimentary cover [Allmendinger et al., 1983]. Seismicity data allows us to examine the response of foreland paleostructures to the modern compressive stresses acting at the eastern margin of the Puna plateau.

Geological field studies by Grier [1990] in the Eastern Cordillera about 100 km south of Jujuy confirmed earlier conclusions that the development of many of the present-day foreland structures has been controlled by the geometry of preexisting structures [Allmendinger et al. 1983, Strecker et al., 1989]. In this area, Neogene deformation has been controlled primarily by the boundaries and internal character of the Cretaceous Salta rift. The subbasins of the Salta rift extend from south of 25.5°S, northward through the region of Jujuy seismicity, and on to the northeast. Through an analysis of surface faulting, facies distribution,

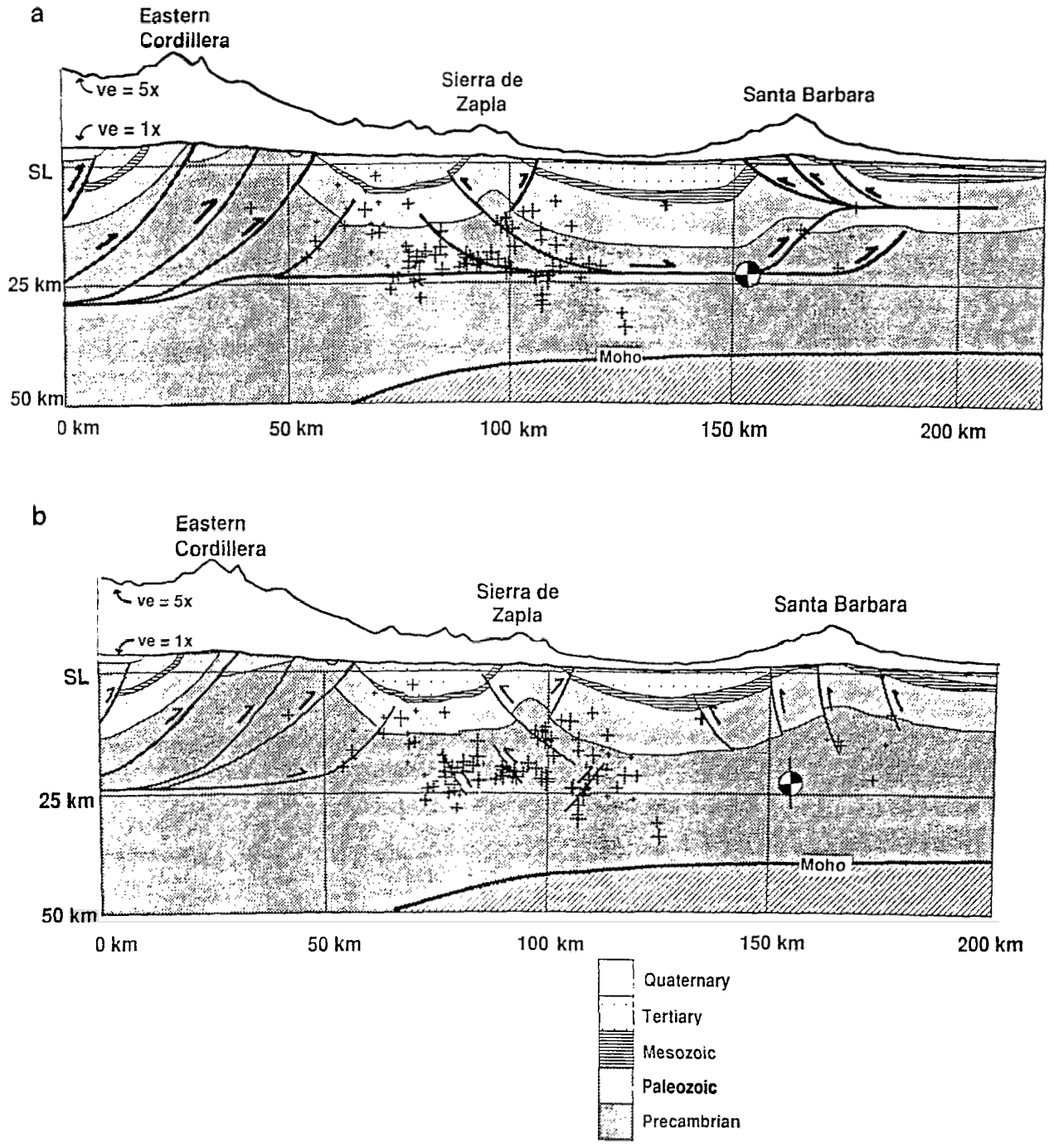

Fig. 12. Interpretations of the seismicity seen in Figure 8c, constrained at surface by lithologic outcrop pattern, mapped faults, and isopachs of Tertiary and Cretaceous units. In both models the seismicity beneath the Eastern Cordillera is interpreted as activity on a west dipping zone of thrusts that bring Precambrian basement in contact with Tertiary at the edge of the high Cordillera. (a) "Thin-skinned" model for structural shortening in the Jujuy segment of the Andean foreland. In this model much of midcrustal activity beneath the Zapla anticline is hypothesized to occur along a detachment surface, with the active nodal planes for 20 to 25-km-deep events being shallow and west dipping. This model is supported by Chinn and Isacks [1983] solution for a mb = 5.6 earthquake, shown here projected sideways into the vertical section. (b) Alternative, "thick-skinned" model. Here the midcrustal activity is hypothesized to occur along higher-angle reverse faults, with the active nodal planes for 20 to25-km-deep events, as well as the event of Chinn and Isacks [1983], being steep and east dipping. In this interpretation, deformation in the Jujuy foreland is similar to that found in the Pampean ranges farther south.

and industry seismic reflection data, Grier reconstructed an east-west cross section at the latitude of 25.5°S, estimating a total shortening of 17% within the last 10-12 m.y. A hypothesized feature of her structural model, along which much of the shortening has been accomplished, is a reactivated detachment surface originally formed during Cretaceous extension. Grier concludes that this midcrustal detachment, along with the bounding and internal faults of the Cretaceous rift, has been reactivated in a reverse sense under the influence of Cenozoic compressional stresses, resulting in an inversion of the rift basin.

The spatial distribution of crustal seismicity, along with the focal mechanism solutions and stress orientation studies, suggests that a variation of Grier's model may also apply in the Jujuy region. Two versions of the model are superimposed on a cross sections of seismicity in Figure 12. The locations of surface lithologic contacts and the position and orientation of faults reaching the surface are used along with contours of Tertiary and Cretaceous basin depths to constrain the structure of the shallower portions of the cross sections [Amengual et al., 1979; Allmendinger et al., 1983, Salfity, 1979]. The only deeper subsurface constraints available are the 42 km depth to the base of the crust, obtained in the present study from Moho-reflected P waves, and an estimated gradient on the Moho, obtained from P-wave arrival time delays observed for events within the subducting Nazca plate [Whitman et al., 1989].

The first interpretation of the seismicity (Figure 12a) includes a set of major west dipping thrusts that separate the Eastern Cordillera from the eastern portion of the foreland and an active detachment beneath the entire region. An upward ramping of the thrust system beneath the Eastern Cordillera may explain the rapid westward increase in average elevation observed in this area. The shallow seismicity beneath the western part of the Sierra de Zapla anticline is interpreted as the western limit of a subbasin of the Salta Rift. The Sierra de Zapla anticline itself is the result of the reactivation in a reverse sense of high-angle normal faults internal to the Cretaceous rift; the evidence for this interpretation is found in the focal mechanisms of the shallower events found near the margins of the anticline, which typically either have high-angle reverse fault mechanisms or are strike-slip mechanisms with a large thrust component.

The common occurrence of nodal planes with shallow westward dips (events 3, 6, 9, 13, 27, 28, and 29 in Figure 9 and Table 3) leads us to interpret much of the deeper seismicity (20-25 km) as part of an active detachment surface or zone of shearing. Lending support to this interpretation is the focal mechanism solution for one of the largest crustal events recorded in the area, the 1973 mb = 5.6 earthquake. This solution, shown projected into the plane of the cross section in Figure 12a, contains one nodal plane that corresponds to a very low-angle west dipping thrust. Farther to the east, another ramp brings Paleozoic strata to the surface in the core of the Santa Barbara anticline; the extent of this ramp is controlled by the lithologic contacts at the surface and local estimates of Tertiary and Cretaceous formation thickness. As no Tertiary or deeper strata break the surface to the east of the Santa Barbara anticline, the detachment system is interpreted as dying out in a 10 km deep blind thrust beneath the western Gran Chaco (Figure 12a).

A structure similar to the one we hypothesize for the Jujuy region has been inferred from seismological evidence for the Lesser Himalaya. The position and focal mechanism solutions of crustal earthquakes at depths of 15-20 km between the Main Central Thrust and the Main Boundary thrusts of the Himalayas define a north dipping detachment, along which the Indian continental crust is thrust beneath the southern part of the Tibetan plateau [Seeber et al., 1981; Ni and Barazangi, 1984; Barazangi, 1989]. As with the Himalayan-Tibetan structure, thrusting of the South American craton westward beneath the high Altiplano-Puna plateau and the resultant thickening of the crust are considered to be major factors in the creation and maintenance of the plateau [Lyon-Caen et al., 1985; Isacks, 1988].

The interpretation of foreland structure presented in Figure 12a is based on seismicity patterns, Grier's model for basin inversion 100 km to the south and, most importantly, on focal mechanism solutions. Recognizing that for any one earthquake we do not know which of the nodal planes represents the actual slip surface, an alternative model is presented. The alternative interpretation, presented in Figure 12b, calls for E-W shortening to occur on the higher-angle, dominantly east dipping reverse faults. Seismic slip is again presumed to occur on reactivated faults. Since the east dipping nodal planes of the focal mechanisms are generally steep, however, the resulting crustal shortening with this thick-skinned geometry is considerably less than would be expected from a model that includes a through-going detachment.

Whether we adopt the thin-skinned or thick-skinned interpretation, the model of basin reactivation still applies. Old planes of weakness resulting from the extension of pre-Neogene basement, whether low angle and continuous or high angle and en echelon, have been reactivated under compression to form the modern geologic structures of the Jujuy foreland.

The absence of seismicity in the crust of the Puna recorded during this experiment and the scarcity of Puna earthquakes found in the historical record do not necessarily favor either interpretation. The Puna may experience lower levels of seismicity than the eastern foreland because of higher heat flow through the plateau. Alternatively, both the Puna and the Eastern Cordillera may be less seismic than the foreland because of their higher elevation. Assuming that across-strike compressive stresses remain relatively constant from west to east, the greater lithostatic stresses in elevated regions would result in smaller deviatoric stresses for the plateau. Much like the situation Suárez et al. [1983] proposed for the foreland east of the Peruvian Altiplano, thrust faulting would be expected to migrate eastward as the vertical stresses in the ranges forming the eastern edge of the plateau increase. Either, or both, of these conditions might be expected to exist for either of the models proposed in Figure 12.

Acknowledgments. The Jujuy seismicity experiment was a collaborative effort involving investigators from Center for Earthquake Research and Information, Cornell University, Office de la Recherche Scientifique et Technique Outre-Mer, and the Instituto de Minería y Geología in Jujuy. The authors wish to acknowledge

specifically the technical field crew: James Bollwerk, Francis Bondoux, and Klaus Bataille. Robert Smalley and Gregory Steiner developed software and hardware, respectively, for the PANDA network. We are grateful to Betty Coira and Waldo Chayle of the Instituto de Minería y Geología for valuable consultations regarding the geology of Jujuy province. We thank Rick Allmendinger, Martha Grier, and others in the Cornell Andes Project for helpful discussion and guidance in the tectonic interpretation of the data. Muawia Barazangi, Robert Smalley, David James, and Andrew Michael provided helpful critical reviews of the manuscript. This study was supported by National Science Foundation grants EAR-8804976 and EAR-9005222.

REFERENCES

Allmendinger, R. W., V. A. Ramos, T. E. Jordan, M. Palma, and B. L. Isacks, Paleogeography and Andean structural geometry, northwest Argentina, *Tectonics*, *2*, 1-16, 1983.

Amengual, R., V. Mendez, A. Navarini, O. Viera, and J. C. Zanettini, Mapa geológico de la República Argentina, Provincias de Salta y Jujuy, scale 1:400,000, Direccion General de Fabricaciones Militares, Buenos Aires, Argentina,1979.

Barazangi, M., Continental collision zones: seismotectonics and crustal structure, in *The Encyclopedia of Solid Earth Geophysics*, edited by D. L. James, Van Nostrand Reinhold and Co., New York, pp. 58-75, 1989.

Barazangi, M., and B. L. Isacks, Spatial distribution of earthquakes and subduction of the Nazca Plate beneath South America, *Geology*, *4*, 686-692, 1976.

Barazangi, M. , W. Pennington, and B. Isacks, Global study of seismic wave attenuation in the upper mantle behind island arcs using pP waves, *J. Geophys. Res.*, *80*, 1079-1092, 1975.

Bevis, M., and B.L. Isacks, Hypocentral trend surface analysis: Probing the geometry of Benioff Zones, *J. Geophys. Res.*, *89*, 6153-6170, 1984.

Caminos, R., Sierras Pampeanas noroccidentales, Salta, Tucumán, Catamarca, La Rioja, y San Juan, in *Segundo Simp. Geol. Argent.*, *1*, pp. 225-292, Academía Nacional de Ciencias, Córdoba, Argentina, 1979.

Castano, J. C., Zonificacion sismica de la Republica Argentina, tech. rep., Inst. Nac. de Prev. Sismica, San Juan, Argentina, 1977.

Chinn, D. S., and B. L. Isacks, Accurate source depths and focal mechanisms of shallow earthquakes in western South America and in the New Hebrides island arc, *Tectonics*, *2*, 529-564, 1983.

Coira, B., J. Davidson, C. Mpodozis, and V. A. Ramos, Tectonic and magmatic evolution of the Andes of northern Argentina and Chile, *Earth Sci. Rev.*, *18*, 303-332, 1982.

Gephart, J. W., Stress and the direction of slip on fault planes, *Tectonics*, *9*, 845-858, 1990.

Grier, M. E., The influence of the Cretaceous Salta rift basin on the development of Andean structural geometries, NW Argentine Andes, Ph.D. dissertation, Cornell University, Ithaca, N. Y., 1990.

Gutenberg, B. and C. F. Richter, *Seismicity of the Earth*, 2nd ed., Princteon University Press, 1954.

Isacks, B. L., Uplift of the central Andean plateau and bending of the Bolivian orocline, *J. Geophys. Res.*, *93*, 3211-3231, 1988.

James, D. E., Plate tectonic model for the evolution of the Central Andes, *Geol. Soc. Am. Bull.*, *82*, 3325-3346, 1971.

Jordan, T. E., and R. N. Alonso, Cenozoic stratigraphy and basin tectonics of the Andes Mountains, 20°-28° south latitude, *AAPG Bull.*, *71*, 49-64, 1987.

Jordan, T. E., B. L. Isacks, R. W. Allmendinger, J. A. Brewer, V. A. Ramos, and C. J. Ando, Andean tectonics related to geometry of subducted Nazca plate, *Geol. Soc. Am. Bull.*, *94*, 341-361, 1983.

Klein, F. W., Hypocenter location program HYPOINVERSE part 1: User's guide to versions 1, 2, 3, and 4, *US Geol. Surv. Open File Rep. 78-694*, 113 pp., 1978.

Klein, F. W., User's guide to HYPOINVERSE, a program for VAX and Professional 350 computers to solve for earthquake locations, *US Geol. Surv. Open File Rep. 85-515*, 36 pp., 1985.

Luetgert, J. H., User's maunual for RAY84/R83PLT, interactive two-dimensional raytracing/ synthetic seismogram package, *US. Geol. Surv. Open File Rep. 88-0238*, 52 pp., 1988.

Lyon-Caen, H., P. Molnar, and G. Suárez, Gravity anomalies and flexure of the Brazilian Shield beneath the Bolivian Andes, *Earth Planet. Sci. Lett.*, *75*, 81-92, 1985.

Marrett, R.A., The Late Cenozoic tectonic evolution of the Puna plateau and adjacent foreland, northwestern Argentina, Ph.D. dissertation, Cornell Univ., Ithaca, N. Y., 1990.

Marrett, R.A., R. Allmendinger, and M. Grier, Kinematic changes during Late Cenozoic deformation of the southern Puna plateau: Argentine Andes, 23°S-27°S latitude: paper presented at 28th Symposium International Geologic Congress, Washington, D.C., USA, July9-19, 1989.

Mingramm, A., A. Russo, A, Pozzo, and L. Casau, Sierras subandinas, in *Segundo Simp. Geol. Argent.*, *1*, pp. 95-138, Academía Nacional de Ciencias, Córdoba, Argentina, 1979.

Ni, J., and M. Barazangi, Seismotectonics of the Himalayan collision zone: Geometry of the underthrusting Indian plate beneath the Himalaya, *J. Geophys. Res.*, *89*, 1147-1163, 1984.

Pardo-Casas, F., and P. Molnar, Relative motion of the Nazca (Farallon) and South American plates since Late Cretaceous time, *Tectonics*, *6*, 233-248, 1987.

Pilger, R. H., Jr., Cenozoic plate kinematics, subduction and magmatism: South American Andes, *J. Geol. Soc. London*, *141*, 793-802, 1984.

Ramos, V. A., T. E. Jordan, R. W. Allmendinger, C. Mpodozis, S. M. Kay, J. M. Cortés, and M. Palma, Paleozoic terranes of the central Argentine-Chilean Andes, *Tectonics*, *5*, 855-880, 1986.

Reasenberg, P., and D. Oppenheimer, FPFIT, FPPLOT and FPPAGE: Fortran computer programs for calculating and displaying earthquake fault-plane solutions, *US Geol. Surv. Open File Rep. 85-739*, 109 pp., 1985.

Roecker, S. W., Velocity structure of the Pamir-Hindu Kush region: Possible evidence of subducted crust, *J. Geophys. Res.*, *87*, 945-959, 1982.

Roecker, S. W., Y. H. Yeh, and Y. B. Tsai, Three-dimensional P and S wave velocity structure beneath Taiwan: Deep structure beneath an arc-continent collision, *J Geophys. Res.*, *92*, 10,547-10,570, 1987.

Roeder, D., Andean-age structure of Eastern Cordillera (Province of La Paz, Bolivia), *Tectonics*, *7*, 23-39, 1988.

Russo, A., A. Serraiotto, Contribución al Conocimiento de la Estratigrafía Terciaria en el Noroeste Argentino, *VII Cong. Geol. Argent.*, *1*, pp. 715-730, Academía Nacional de Ciencias, Buenos Aires, Argentina, 1979.

Salfity, J. A., Paleogeología de la Cuenca del Grupo Salta (Cretacico-Eogenico) del norte de Argentina, Actas I, *VII Cong. Geol. Argent.*, *1*, pp. 505-515, Academía Nacional de Ciencias, Buenos Aires, Argentina, 1979.

Salfity, J. A., E. M. Brandon, C. R. Monaldi, and E. F. Gallardo, Tectonica compresiva Cuartemaria en la Cordillera Oriental Argentina, latidud de Tilcara (Jujuy), *IX Cong. Geol. Argent.*, *2*, pp. 427-434 Academía Nacional de Ciencias, Buenos Aires, Argentina, 1984.

Seeber, L., J. Armbruster, and R. Quitmeyer, Seismicity and continental subduction in the Himalayan arc, in *Zagros, Hindu Kush, Himalaya, Geodynamic Evolution*, Geodyn. Ser., vol. 3, edited by H. K. Gupta and E. M. Delaney, 215-242, AGU, Washington, D.C., 1981.

Sheffels, B., B. C. Burchfiel, and P. Molnar, Deformational style and crustal shortening in the Bolivian Andes (abstract), *EOS Trans. AGU*, *67*, 1241, 1986.

Smalley, R. F., Jr., and B. L. Isacks, Seismotectonics of thin and thick-skinned deformation in the Andean foreland from local network data: Evidence for a seismogenic lower crust, *J. Geophys. Res.*, *95*, 12,487-12,498, 1990.

Strecker, M. R., P. Cerveny, A. L. Bloom, and D. Malizia, Late Cenozoic tectonism and landscape development in the foreland of the Andes: Northern Sierras Pampeanas (26° - 28° S), Argentina, *Tectonics*, *8*, 517-534, 1989.

Suárez, G. E., P. Molnar, and B. C. Burchfiel, Seismicity, fault plane solutions, depth of faulting, and active tectonics of the Andes of Peru, Equador, and southern Columbia, *J. Geophys. Res.*, *88*, 10,403-10,428, 1983.

Turner, J. C. M., and V. Mendez, Puna, in *Segundo Simp. Geol. Argent.*, *1*, pp. 13-56, Academía Nacional de Ciencias, Córdoba, Argentina, 1979.

Wdowinski, S., R. J. O'Connell, and P. England, A continuum model of continental deformation above subduction zones: Application to the Andes and the Aegean, *J. Geophys. Res.*, *94*, 10,331-10,346, 1989.

Whitman, D., T. Cahill, B. Isacks, J. L. Chatelain, A. Perez, J. M. Chiu, Crustal structure along the eastern edge of the Altiplano-Puna plateau, NW Argentina: A synthesis of seismic, gravity and topographic data (abstract), *EOS Trans. AGU*, *70*, 1361, 1989.

T. Cahill, Engineering Tectonics, P.A., P.O. Box 4798, Winston-Salem, NC 27115-4798.

J.-L. Chatelain, Office de la Recherche Scientifique et Technique Outre-Mer, IRIGM-LGIT, Universite J. Fourier, BP53X, 38041, Grenoble Cedex , France.

J. M. Chiu, Center for Earthquake Research and Information, 3904 Central Avenue, Memphis, TN 38152.

B. L. Isacks and D. Whitman, Department of Geological Sciences, Cornell University, Ithaca, NY 14853.

A. Perez, Instituto de Minería y Geología, Universidad Nacional de Jujuy, 5400 San Salvador de Jujuy, Argentina.

(Received October 15, 1990;
revised December 20, 1991;
accepted January 30, 1992.)